JCI The Journal of Clinical Investigation

The loss-of-function PCSK9^{Q152H} variant increases ER chaperones GRP78 and GRP94 and protects against liver injury

Paul F. Lebeau, Hanny Wassef, Jae Hyun Byun, Khrystyna Platko, Brandon Ason, Simon Jackson, Joshua Dobroff, Susan Shetterly, William G. Richards, Ali A. Al-Hashimi, Kevin Doyoon Won, Majambu Mbikay, Annik Prat, An Tang, Guillaume Paré, Renata Pasqualini, Nabil G. Seidah, Wadih Arap, Michel Chrétien, Richard C. Austin

J Clin Invest. 2021;131(2):e128650. https://doi.org/10.1172/JCI128650.

Research Article | Hepatology | Vascular biology

Graphical abstract

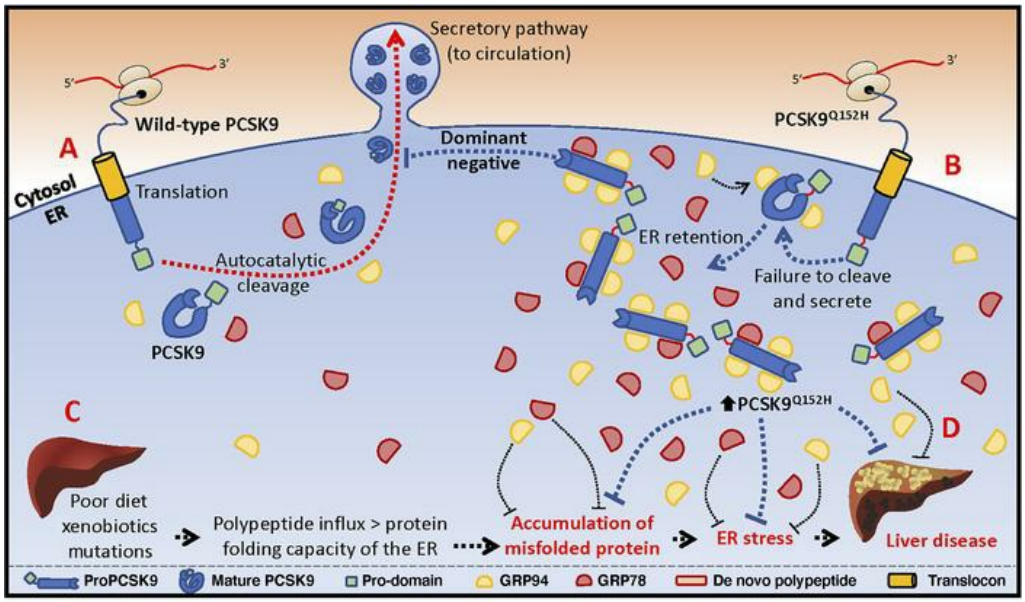

Find the latest version:

https://jci.me/128650/pdf

The loss-of-function PCSK9^{Q152H} variant increases ER chaperones GRP78 and GRP94 and protects against liver injury

Paul F. Lebeau,[1] Hanny Wassef,[2] Jae Hyun Byun,[1] Khrystyna Platko,[1] Brandon Ason,[3] Simon Jackson,[3] Joshua Dobroff,[4] Susan Shetterly,[3] William G. Richards,[5] Ali A. Al-Hashimi,[1] Kevin Doyoon Won,[1] Majambu Mbikay,[2] Annik Prat,[6] An Tang,[7] Guillaume Paré,[8] Renata Pasqualini,[9] Nabil G. Seidah,[6] Wadih Arap,[10] Michel Chrétien,[2] and Richard C. Austin[1]

[1]Department of Medicine, McMaster University, The Research Institute of St. Joe's Hamilton and Hamilton Centre for Kidney Research, Hamilton, Ontario, Canada. [2]Laboratory of Functional Endoproteolysis, Clinical Research Institute of Montreal, affiliated with the University of Montreal, Montreal, Quebec, Canada. [3]Cardiometabolic Disorders, Amgen Research Inc., South San Francisco, California, USA. [4]Bristol Myers Squibb, Redwood City, California, USA. [5]23andMe, South San Francisco, California, USA. [6]Laboratory of Biochemical Neuroendocrinology, Clinical Research Institute of Montreal, affiliated with the University of Montreal, Montreal, Quebec, Canada. [7]Department of Radiology at the Centre Hospitalier Universitaire de Montréal, University of Montreal, Montreal, Quebec, Canada. [8]Population Health Research Institute and Departments of Medicine, Epidemiology, and Pathology, McMaster University, Hamilton, Ontario, Canada. [9]Division of Cancer Biology, Department of Radiology Oncology, and [10]Division of Hematology/Oncology, Department of Medicine, Rutgers New Jersey Medical School and Rutgers Cancer Institute of New Jersey, Newark, New Jersey, USA.

Individuals harboring the loss-of-function (LOF) proprotein convertase subtilisin/kexin type 9 Gln152His variation (PCSK9^{Q152H}) have low circulating low-density lipoprotein cholesterol levels and are therefore protected against cardiovascular disease (CVD). This uncleavable form of proPCSK9, however, is retained in the endoplasmic reticulum (ER) of liver hepatocytes, where it would be expected to contribute to ER storage disease (ERSD), a heritable condition known to cause systemic ER stress and liver injury. Here, we examined liver function in members of several French-Canadian families known to carry the PCSK9^{Q152H} variation. We report that PCSK9^{Q152H} carriers exhibited marked hypocholesterolemia and normal liver function despite their lifelong state of ER PCSK9 retention. Mechanistically, hepatic overexpression of PCSK9^{Q152H} using adeno-associated viruses in male mice greatly increased the stability of key ER stress-response chaperones in liver hepatocytes and unexpectedly protected against ER stress and liver injury rather than inducing them. Our findings show that ER retention of PCSK9 not only reduced CVD risk in patients but may also protect against ERSD and other ER stress–driven conditions of the liver. In summary, we have uncovered a cochaperone function for PCSK9^{Q152H} that explains its hepatoprotective effects and generated a translational mouse model for further mechanistic insights into this clinically relevant LOF PCSK9 variant.

Introduction

Circulating low-density lipoprotein cholesterol (LDLc) is a major driver in the development and progression of cardiovascular disease (CVD) (1–3). In the blood, LDLc is largely regulated by proprotein convertase subtilisin/kexin type 9 (PCSK9), a secreted serine protease that enhances the degradation of hepatic LDL receptor (LDLR) (4–6). While gain-of-function mutations in *PCSK9* are associated with elevated serum LDLc levels and premature CVD, loss-of-function (LOF) *PCSK9* mutations confer a hypocholesterolemic phenotype with reduced CVD risk (4, 7–10). LOF mutations in the serine protease catalytic domain (e.g., PCSK9^{S386A}) or in the site of autocatalytic processing of PCSK9, Gln$^{152}\downarrow$ (e.g., PCSK9^{Q152H}), fail to undergo autocatalytic cleavage and maturation in the endoplasmic reticulum (ER). As a result, PCSK9 is retained in this cellular compartment and thus unable to degrade the LDLR (8, 9).

The ER is the largest organelle in secretory cells, including liver hepatocytes, and is the major site of Ca^{2+} storage and lipid and carbohydrate metabolism, as well as de novo protein folding (11–13). The retention of inactive or misfolded proteins in the ER can lead to ER stress (14–19), and a wide range of heritable LOF mutations in proteins that transit the ER are retained in this organelle and contribute to ER storage disease (ERSD). To mitigate or resolve ER stress, the unfolded protein response (UPR) drives the expression of ER-resident molecular chaperones, such as the glucose-regulated proteins of 78 and 94 kDa (GRP78 and GRP94) (20, 21).

ER stress is a well-known driver of liver disease and its complications (13, 22, 23). Chronic UPR activation promotes apoptosis, inflammation, and fibrosis, all of which contribute to terminal hepatic disease, commonly resulting in liver cirrhosis and/or cancer. We reasoned that while LOF variants of PCSK9 were protective against CVD over a lifetime, the prolonged accumulation of these proteins in the ER of hepatocytes in humans may contribute to chronic liver disease. Although it is well known that individuals with the LOF PCSK9^{Q152H} variation exhibit reduced CVD risk,

Authorship note: PFL and HW contributed equally to this work.
Conflict of interest: BA, SS, and SJ are employees of Amgen and hold Amgen stock. RCA is on the Scientific Advisory Board of Precision BioLogic Inc.
Copyright: © 2021, American Society for Clinical Investigation.
Submitted: March 6, 2019; **Accepted:** November 3, 2020; **Published:** January 19, 2021.
Reference information: *J Clin Invest*. 2021;131(2):e128650.
https://doi.org/10.1172/JCI128650.

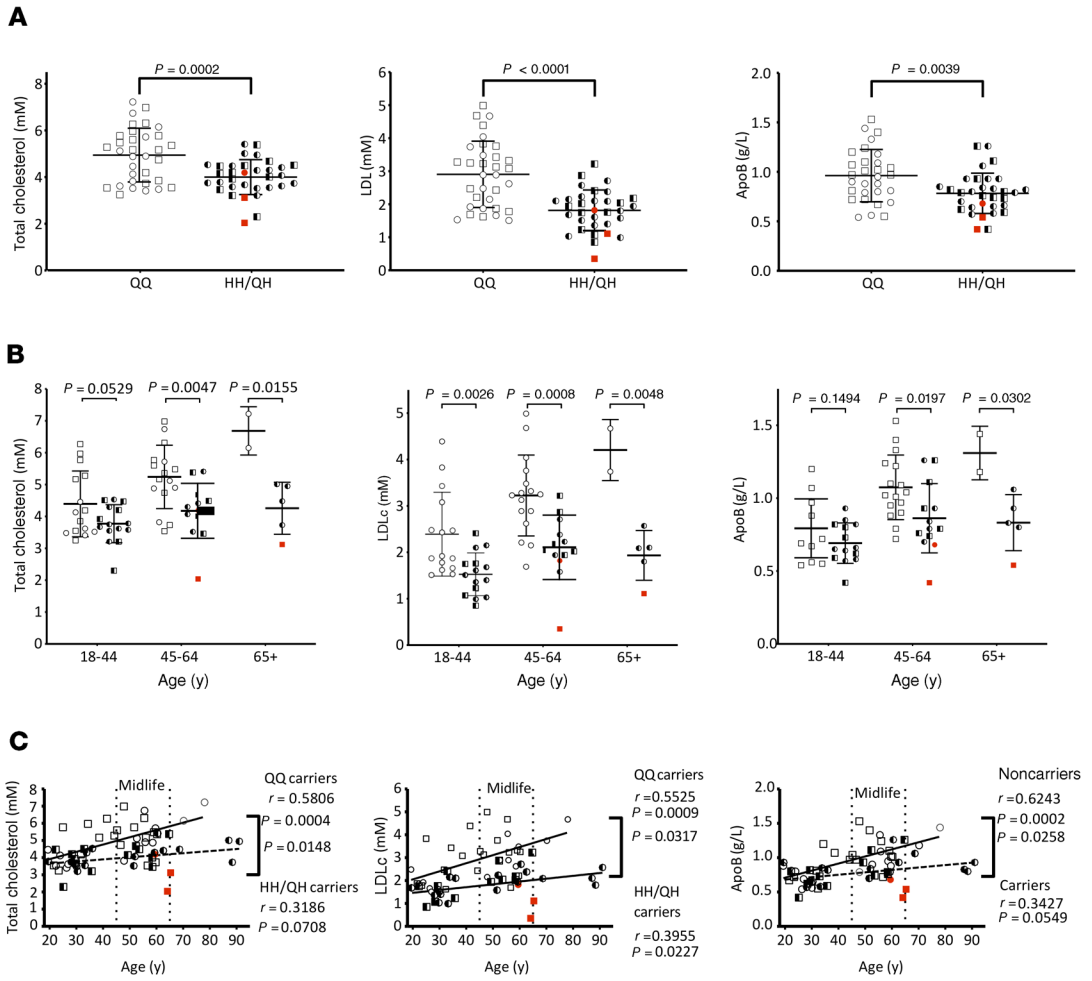

Figure 1. Assessment of circulating lipid levels in carriers of the PCSK9^{Q152H} variation. (**A**) Total cholesterol, cLDL, and ApoB levels were quantified in homozygous and heterozygous carriers (HH and QH, respectively) of the PCSK9^{Q152H} variation and compared with those in noncarrier family members (QQ). (**B** and **C**) Total cholesterol, LDLc, and ApoB data were further stratified to age-dependence. Data are presented as mean ± SD. Unpaired, 2-tailed Student's *t* tests. (**A** and **B**) and regression analysis (**C**) were used to determine statistical differences between groups.

the impact of lifelong ER retention of this PCSK9 variant in liver hepatocytes has not yet been examined'

Notably, we among others have previously reported that ER-resident chaperones are capable of directly interacting with PCSK9, thereby affecting its secretory status, as well as its ability to trigger conventional UPR signaling cascades (24, 25). The purpose of this study was twofold: (a) to determine whether ER retention of PCSK9 leads to chronic ER stress and liver injury in mice or in humans, and (b) to further characterize the intracellular role(s) of PCSK9 as a putative binding partner and cochaperone within the ER of hepatocytes.

Results

Clinical attributes and circulating cholesterol levels in human subjects harboring the PCSK9^{Q152H} variation. A unique cohort of human subjects (N = 66) was assembled from 3 of the 4 French-Canadian families known to harbor the LOF PCSK9^{Q152H} variation (8, 10), including homozygote carriers (HH; N = 3), heterozygote carriers (QH; N = 30), and wild-type (WT) noncarrier family siblings (QQ; N = 33). Full medical examination as well as an assessment of blood biochemistry was carried out in these subjects. The blood chemistry of homozygous carriers was similar to that of heterozygous carriers, aside from the absence of detectable plasma PCSK9 in the homozygotes (Supplemental Table 1; supplemental material available online with this article; https://doi.org/10.1172/JCI128650DS1). The 2 genotypic cohorts (HH/QH vs. QQ) had similar distributions of age, sex, body mass index (BMI), and blood pressure. Consistent with previous LOF PCSK9 variations, these subjects also demonstrated marked reductions in circulating levels of total cholesterol (TC), LDLc, and apolipoprotein B (ApoB) (Figure 1A). Stratification of these data demonstrated that, while LDLc differed substantially between carriers and noncarriers in all 3 age groups, TC and ApoB did so only during and after midlife (Figure 1B). Further stratification revealed that TC, LDLc, and ApoB increased with age in noncarriers at a significantly greater rate than in PCSK9^{Q152H} carriers (Figure 1C; P = 0.0148, 0.0317, and 0.0258, respectively). In contrast, no significant differences in circulating high-density lipoprotein or triglycerides were observed between carriers and noncarriers (Supplemental Figure 1). Similarly, pooling of the carrier and noncarrier groups also confirmed that circulating PCSK9 levels strongly correlated with TC, LDLc, and ApoB (Supplemental Figure 2; P = 0.0004, 0.0006, and

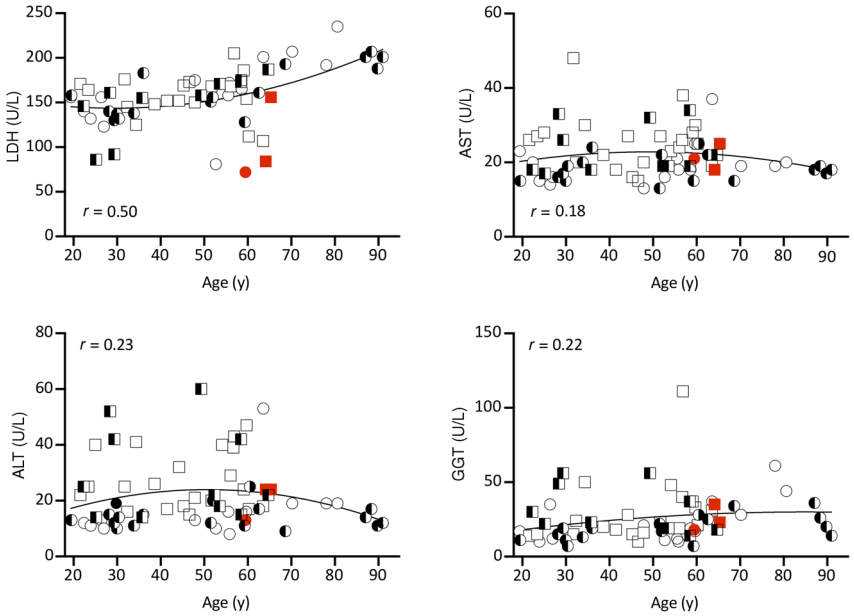

Figure 2. Liver function in PCSK9^{Q152H}-expressing subjects and family controls. Correlations between age and the circulating liver enzymes lactate dehydrogenase (LDH), aspartate aminotransferase (AST), alanine aminotransferase (ALT), and γ-glutamyl transpeptidase (GGT) for carriers of the PCSK9^{Q152H} variant and family member controls. Squares represent men; circles represent women. Homozygous Q152H subjects (HH) are in red, heterozygous Q152H (QH) subjects are half black, and family controls (QQ) are in white. Second-order quadratic correlation is shown for the entire cohort. All data are presented as mean ± SD and were analyzed by unpaired, 2-tailed Student's *t* test.

0.0035, respectively) but not with either lipoprotein(a) or soluble LDLR (sLDLR; $P = 0.3947$ and 0.1576).

Liver function in subjects harboring the PCSK9^{Q152H} variation. It is well established that LOF variations in PCSK9 incur a state of hypocholesterolemia (8–10). However, the toxicological impact of ER PCSK9 retention in the liver over a lifetime has not yet been examined. To assess liver function in subjects harboring the PCSK9^{Q152H} variant, we assessed circulating liver enzymes, including lactate dehydrogenase (LDH), aspartate aminotransferase (AST), alanine aminotransferase (ALT), and γ-glutamyl transpeptidase (GGT), which reside within liver hepatocytes under normal conditions. We found no increase in subjects expressing the PCSK9^{Q152H} variation compared with noncarrier controls (Figure 2). This is indicative of normal liver function and absence of injury. Among the older individuals, PCSK9^{Q152H}-expressing subjects ($N = 6$), including homozygotes ($N = 2$) and heterozygotes ($N = 4$), along with WT family controls ($N = 7$) underwent abdominal MRI for further imaging-based analysis. Consistent with the liver enzyme data, liver volume and fat content, which are early stage markers of liver disease, were not different in subjects with or without the PCSK9^{Q152H} variation (Table 1). Because PCSK9 is also expressed in the kidney (5), renal function was examined via quantification of estimated glomerular filtration rate (eGFR). Like liver function, eGFR was not significantly different between PCSK9^{Q152H} carriers and family controls (Supplemental Figure 3).

Design, generation, and functional characterization of Pcsk9$^{-/-}$ mice overexpressing PCSK9^{Q152H} or LDLR^{G544V}. To more directly study the retention of LOF PCSK9 in the ER and how that might affect liver function, we expressed the PCSK9^{Q152H} mutation in the livers of male *Pcsk9*$^{-/-}$ mice on the C57BL/6J background via adeno-associated virus–mediated (AAV-mediated) transduction (26). The AAV constructs used in these studies encoded either human PCSK9^{WT} (AAV-hPCSK9^{WT}), human PCSK9^{Q152H} (AAV-hPCSK9^{Q152H}), or human LDLR^{G544V} (AAV-hLDLR^{G544V}). Importantly, previous studies have demonstrated that the retention of LDLR^{G544V} in cultured cells causes robust ER stress; thus, treatment with AAV-hLDLR^{G544V} served as a positive control in our studies (27). Finally, treatment with an AAV encoding empty vector (AAV-EV) served as the negative control. To confirm the appropriate expression and localization of these proteins, livers were assessed by immunohistochemical (IHC) staining and immunoblots. Treatment with AAV-hPCSK9^{Q152H} caused a significant increase in PCSK9 staining in the ER compared with the AAV-hPCSK9^{WT} treatment (Figure 3, A–C). Notably, a distinct expansion of the ER was also apparent in hepatocytes exposed to AAV-hPCSK9^{Q152H} compared with those exposed to AAV-hPCSK9^{WT}, a phenomenon commonly associated with ER stress.

The secretory status of the different PCSK9 constructs was assessed by either human (Figure 3D) or mouse (Figure 3E) PCSK9 ELISAs. Treatment of *Pcsk9*$^{-/-}$ mice with AAV-hPCSK9^{WT} led to an approximately 15-fold increase in circulating PCSK9 levels compared with AAV-hPCSK9^{Q152H} (32.6 vs. 2.2 μg/mL) (Figure 3D) and an approximately 113-fold increase compared with endogenously expressed mouse PCSK9 in C57BL/6J mice (32.6 vs. 0.289 μg/mL) (Figure 3E). To determine whether it was the uncleaved proPCSK9 (~75 kDa) accumulating in the livers of AAV-hPCSK9^{Q152H}–treated mice, we next analyzed their expression levels by immunoblotting. A significant accumulation of proPCSK9, compared with the mature autocatalytically cleaved PCSK9 (~63 kDa), was present in the livers of AAV-hPCSK9^{WT}–treated mice (Figure 3F). The positive control hLDLR^{G544V} also accumulated an immature form (LDLR-I; ~100 kDa) in the livers of mice. Consistent with these findings, IHC staining revealed increased intracellular human LDLR in the livers of mice treated with AAV-hLDLR^{G544V} compared with the other groups (Supplemental Figure 4). A marked reduction in endogenously expressed hepatic cell surface mouse LDLR (Figure 3, G and H) and an increase in plasma triglyceride (Figure 3I) and cholesterol (Figure 3J) levels in AAV-hPCSK9^{WT}–treated mice compared with those treated with AAV-hPCSK9^{Q152H} also confirmed the functionality of these human transgenes in our mouse models (28).

Hepatic ER retention of PCSK9^{Q152H} increases the abundance of liver ER stress-response chaperone proteins GRP78 and GRP94. Together, our human and mouse data demonstrate that the LOF PCSK9^{Q152H} variant strongly accumulates in an uncleaved form in the ER of liver hepatocytes, causes substantial expansion of this organelle, but paradoxically does not seem to negatively affect

Table 1. Liver MRI in subjects harboring the PCSK9^{Q152H} mutation

Patient number	PCSK9^{Q152H}	Age	BMI	Liver fat fraction (%)	Liver volume (mL)
1	HH	64.2	30.2	10.40	1835.00
2	HH	65.3	24.8	4.00	1371.00
Mean	**HH**	**64.7**	**27.5**	**7.2**	**1603**
SD	**HH**	**0.8**	**3.8**	**4.5**	**328.1**
3	QH	89.8	24.6	3.20	1023.00
4	QH	88.4	23.7	4.10	1113.00
5	QH	64.7	22.2	4.70	1780.00
6	QH	62.6	21.2	4.00	1134.00
Mean	**QH**	**76.4**	**22.9**	**4**	**1262.5**
SD	**QH**	**14.7**	**1.5**	**0.6**	**348.3**
7	QQ	80.6	32.0	8.70	1493.00
8	QQ	78.0	28.1	22.80	1206.00
9	QQ	70.2	24.8	2.80	1318.00
10	QQ	63.6	27.7	16.20	1598.00
11	QQ	63.5	26.0	4.90	1744.00
12	QQ	56.9	40.4	10.40	1875.00
13	QQ	58.6	26.7	1.50	1217.00
Mean	**QQ**	**67.3**	**29.4**	**9.6**	**1493**
SD	**QQ**	**9.2**	**5.4**	**7.7**	**261.1**

HH, homozygote carrier; QH, heterozygote carrier; QQ, noncarrier sibling.

liver function. This counterintuitive finding suggests that there may be a compensatory mechanism triggered by the ER accumulation to protect the liver. PCSK9 has been shown to interact directly with GRP78 and GRP94 (24, 25), which are both ER-resident chaperones known to play central roles in the regulation of protein folding and UPR activation (29). We first assessed the levels and localization of these proteins by IHC staining and immunoblots. Overexpressing the PCSK9^{Q152H} variant in the livers of mice significantly increased both GRP78 and GRP94 proteins to levels comparable to those in mice treated with the strong ER stress–inducing agent tunicamycin (TM) (Figure 4, A–C). A similar increase in GRP78 and GRP94 levels was also observed in the livers of mice treated with the other ER-accumulating variant, AAV-hLDLR^{G544V}. Staining with an anti-KDEL antibody, which detects both GRP94 and GRP78, demonstrated a similar increase in the livers of AAV-hPCSK9^{Q152H}– and AAV-hLDLR^{G544V}–treated mice (Supplemental Figure 5). Thus, hPCSK9^{Q152H} and hLDLR^{G544V}, which both accumulate in the ER, also appear to increase the protein abundance of GRP78 and GRP94.

Further analysis revealed that AAV-hLDLR^{G544V}–treated mice had a significant increase in mRNA levels of these ER chaperones whereas AAV-hPCSK9^{Q152H}–treated counterparts did not (Figure 4D). A comparison of the livers from AAV-hLDLR^{G544V}–treated mice with those of C57BL/6J mice treated with the ER stress–inducing agent TM (250 μg/kg, 24 hours) also revealed a similar relocalization of GRP78 from the ER to the cell surface of hepatocytes, a hallmark of prolonged ER stress (30–33) known to contribute to hepatocellular carcinoma as well as endothelial cell activation and atherosclerosis (Supplemental Figure 6). Immunoprecipitation experiments demonstrated interaction between GRP78 and GRP94 with LOF hPCSK9^{Q152H} but not with the WT hPCSK9 in mouse livers (Supplemental Figure 7A). As an alternative approach to induce PCSK9 accumulation in the ER, we also overexpressed GRP78 and GRP94. In support of our findings, this overexpression has previously been shown to block PCSK9 secretion owing to a direct interaction between the proteins in the ER (29); this also increased LDL uptake in human liver cancer HepG2 cells (Supplemental Figure 7B).

To gain additional insights into the effect of PCSK9 on GRP78 and GRP94 stability, *Pcsk9*$^{-/-}$ and age-matched *Pcsk9*$^{+/+}$ control mice were fed an ER stress–inducing high-fat diet (HFD) for 12 weeks (22). In a reciprocal manner to increased ER PCSK9 levels, as is the case in hepatocytes exposed to AAV-hPCSK9^{Q152H}, hepatic PCSK9 deficiency led to an attenuation of HFD-induced GRP78 and GRP94 protein levels, in comparison with *Pcsk9*$^{+/+}$ controls (Figure 4, E and F, and Supplemental Figure 8A). As in AAV-treated mice, real-time PCR demonstrated that changes in the expression of GRP78 and GRP94 in HFD-fed *Pcsk9*$^{-/-}$ mice were restricted to the protein level (Supplemental Figure 8B).

ER retention of PCSK9 protects cultured hepatocytes from ER stress and cytotoxicity. Given that ER retention of PCSK9^{Q152H} increased the protein abundance of key ER stress-response chaperones, our next aim was to determine whether expression of PCSK9^{Q152H} could protect against ER stress. To gain functional insight into that possibility, we transfected human embryonic kidney (HEK293) cells with mammalian expression vectors encoding either human PCSK9^{WT} or PCSK9^{Q152H} for 48 hours and treated them with an ER stress–inducing agent, TM (2 μg/mL) or thapsigargin (TG; 100 nM), for an additional 24 hours. As expected, treatment of PCSK9^{WT}-expressing cells with ER stress–inducing agents led to a strong increase in mRNA expression of the ER stress markers GRP78, sXBP1, IRE1α, and ATF6, as determined by real-time PCR (Figure 5A). This effect, however, was repressed in cells expressing PCSK9^{Q152H}, strongly suggesting that PCSK9^{Q152H}

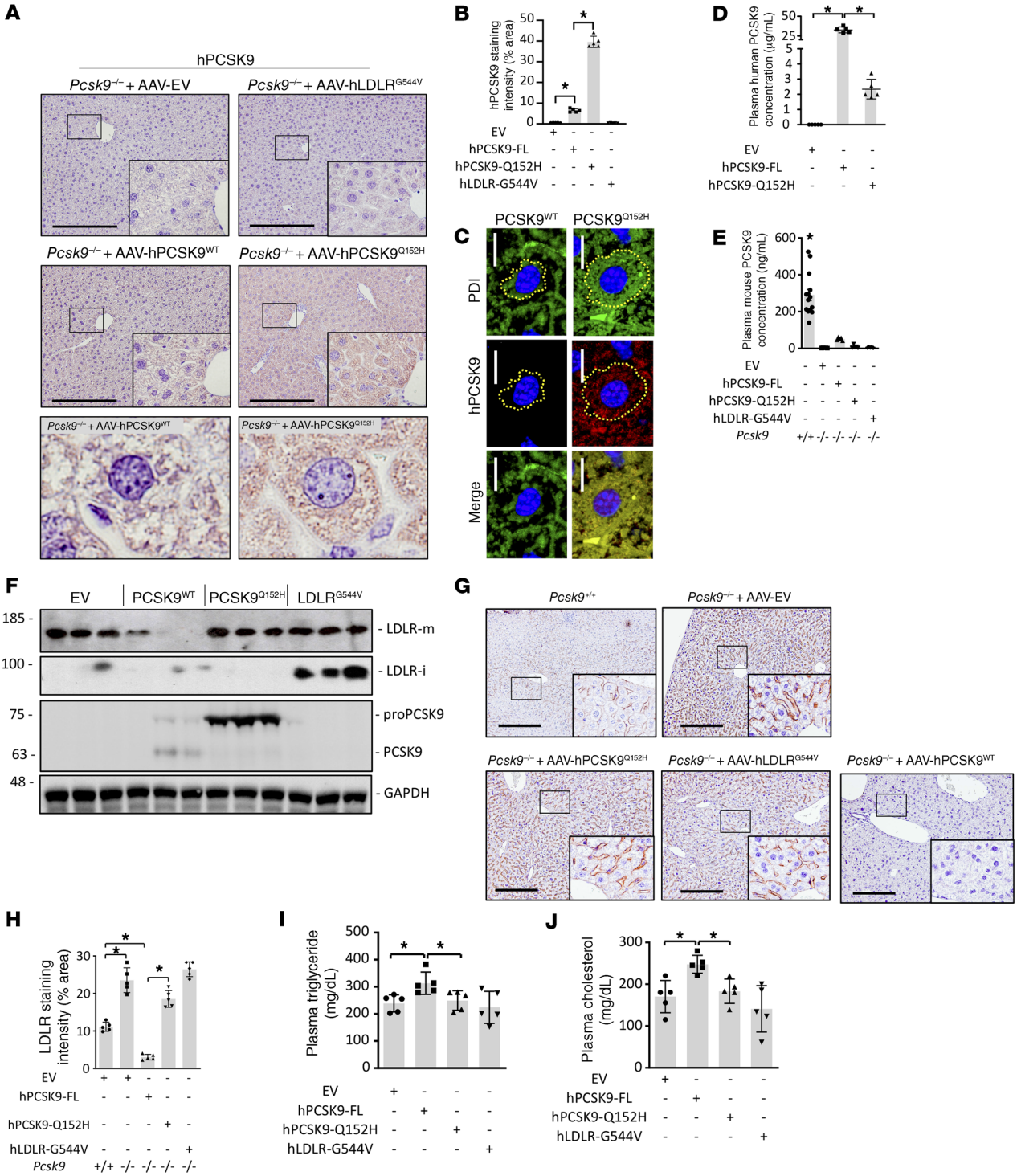

Figure 3. Characterization of PCSK9/LDLR AAV–treated mice. *Pcsk9*$^{-/-}$ mice (n = 5) were treated with AAV encoding empty vector (EV), human (h) PCSK9 WT, or ER-retained variants hPCSK9^{Q152H} and hLDLR^{G544V}. (**A** and **B**) Intracellular PCSK9 expression and retention were assessed via IHC staining and quantification using ImageJ software. (**C**) Immunofluorescent staining of PCSK9 and the ER marker protein disulfide isomerase (PDI) was also used to visualize ER PCSK9 retention and expansion (ER area depicted as yellow dotted line). (**D** and **E**) Secreted PCSK9 levels were examined using human (**D**) and mouse (**E**) PCSK9 ELISAs. (**F**) Liver expression of immature LDLR (LDLR-i; 100 kDa) and proPCSK9 (75 kDa) was confirmed via immunoblots. (**G**–**J**) Additional parameters known to be modulated by secreted PCSK9, including cell surface hepatic LDLR expression (**G** and **H**), plasma triglyceride levels (**I**), and plasma cholesterol levels (**J**), were also examined. Values are represented as mean ± SD. *$P < 0.05$. ANOVA was used for all statistical comparisons (**A**–**J**). Scale bars: **A** and **G**, 200 μm; **C**, 10 μm. Original magnification, ×60 (**A**, lower panels).

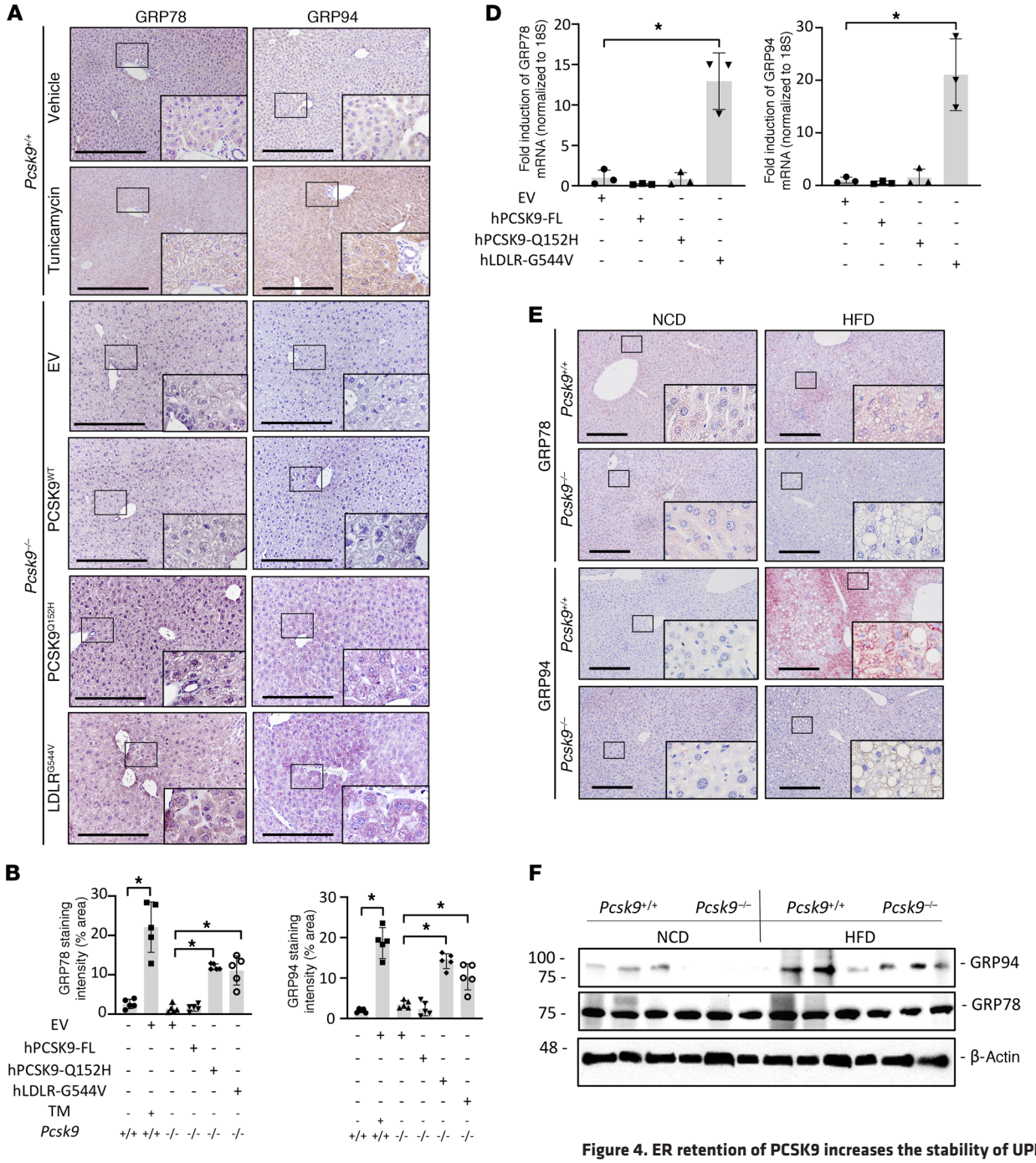

Figure 4. ER retention of PCSK9 increases the stability of UPR chaperones GRP78 and GRP94. (**A**) The livers of *Pcsk9*$^{-/-}$ mice (n = 5) treated with AAV encoding EV, hPCSK9 WT, and ER-retained variant hPCSK9^{Q152H} or hLDLR^{G544V} were examined for expression of ER-resident chaperones GRP78 and GRP94 by IHC staining. (**B**) Relative staining intensities were quantified using ImageJ software. (**C** and **D**) GRP78 and GRP94 protein and mRNA levels were also assessed using immunoblots and real-time PCR. (**E** and **F**) *Pcsk9*$^{-/-}$ mice and age-matched *Pcsk9*$^{+/+}$ controls (n = 5) were fed either normal chow diet (NCD) or high-fat diet (HFD) for 12 weeks and examined for GRP78 and GRP94 expression by IHC staining and immunoblots. Values are represented as mean ± SD. ANOVA was used for all statistical comparisons (**A**–**F**). *$P < 0.05$. Scale bars: **A** and **E**, 200 μm.

inhibits the UPR. To further assess this, we transfected HuH7 immortalized human hepatocytes with either PCSK9^{Q152H} or PCSK9^{WT}. Indeed, we observed a significant reduction in the expression of key transducers of the UPR, phosphorylated PERK (p-PERK) and IRE1α, at the protein level in PCSK9^{Q152H}-transfected versus PCSK9^{WT} control cells (Figure 5B). HepG2 human hepatocytes transduced with PCSK9^{Q152H} also exhibited a reduction in cytotoxicity, in both the absence and the presence of TG or TM, compared with those transfected with PCSK9^{WT} (Figure 5C). To determine whether the protective effect of ER PCSK9 retention was dependent on GRP94, we repeated the experiment in HepG2 cells treated with siRNA targeted against GRP94 (siGRP94). Following reduced GRP94 expression, ER PCSK9 retention substantially increased cytotoxicity in comparison with cells expressing the secreted PCSK9^{WT} in the presence or absence of either TM or TG (Figure 5D). In a reciprocal manner, siRNA-mediated knockdown of PCSK9 also contributed to TG-induced cytotoxicity in HEK293, HepG2, and HuH7 cells (Figure 5E).

Thus, PCSK9^{Q152H} is retained in the ER, inhibits the UPR, and can attenuate ER stress–induced cytotoxicity likely by upregulating GRP78 and GRP94. To test this hypothesis directly, we examined the effect of overexpressing GRP78 and GRP94 on ER stress–induced cytotoxicity in HepG2 cells. Consistent with cells overexpressing PCSK9^{Q152H}, those overexpressing GRP78 or GRP94 were protected against TG- or TM-induced cell death (Figure 5, F and G). Finally, to determine whether the expression of PCSK9^{Q152H} confers general protection against ER stress–induced cytotoxicity caused by misfolded protein variants, HepG2 cells were cotransfected with native secreted WT vasopressin (VP^{WT}) or an ER-retained VP^{G17V} variant that was previously shown to cause ER stress and cytotoxicity in a variety of cell lines (16, 25). Similarly to previous studies, we observed that the retention of VP^{G17V} in the ER markedly increased cytotoxicity. This effect was attenuated by the coexpression of ER-retained PCSK9^{Q152H} (Figure 5H). These findings were also confirmed by terminal deoxynucleotidyl transferase dUTP nick end labelling (TUNEL) assay, which stains damaged DNA resulting from apoptosis (Figure 5, I and J). The expression/inhibition of PCSK9, GRP94, GRP78, and VP in HepG2 cells transfected with mammalian expression vectors or siRNA was confirmed by immunoblot analysis (Figure 5K). Together with our observations in mice, these in vitro findings indicate that ER retention of PCSK9 increases the protein abundance of ER stress-response chaperones. Additionally, in a manner dependent on the stress-response chaperones, ER-retained PCSK9 protects against ER stress and cytotoxicity in cultured cells.

ER retention of LDLR^{G544V}, but not PCSK9^{Q152H}, leads to robust hepatic ER stress. Although both the LDLR^{G544V} and PCSK9^{Q152H} accumulate in the ER, only AAV-hLDLR^{G544V} induces the UPR. Thus far, we showed that GRP78 and GRP94 are upregulated at both the protein and mRNA levels in mice expressing hLDLR^{G544V}, but only at the protein level in mice expressing hPCSK9^{Q152H}, and that hPCSK9^{Q152H} can bind GRP78 and GRP94. We therefore reasoned that ER-retained PCSK9^{Q152H} binds to these chaperones and increases their stability, while ER retention of LDLR^{G544V} induces a UPR-mediated increase in their expression. Supporting this mechanistic model, we found increased expression of the ER stress markers p-PERK, PERK, IRE1α, sXBP1, p-eIF2α, ATF4, and CHOP specifically in the livers of AAV-hLDLR^{G544V}–treated mice, and not in AAV-hPCSK9^{Q152H}– or AAV-hPCSK9^{WT}–treated mice (Figure 6, A and B). IHC staining also revealed increased expression of the ER stress markers p-PERK and p-IRE1α in the livers of AAV-hLDLR^{G544V}–treated mice compared with AAV-hPCSK9^{Q152H}, as well as AAV-hPCSK9^{WT} and AAV-EV (Figure 6C). Moreover, the accumulation of misfolded protein aggregates resulting from ER stress was also examined by thioflavin-S staining (Supplemental Figure 9) and demonstrated an increase in staining intensity specifically in AAV-hLDLR^{G544V}–treated mice. Thus, hLDLR^{G544V} retention in the ER, but not hPCSK9^{Q152H} ER retention, triggers the UPR. Finally, we examined the effect of ER stress by ER-retained hLDLR^{G544V} on liver function by quantifying serum ALT activity. Despite significant retention of PCSK9 in the livers of AAV-hPCSK9^{Q152H}–treated mice, liver injury was only observed in mice treated with AAV-hLDLR^{G544V} (Figure 6D).

Prolonged and/or chronic UPR activation causes apoptosis, which contributes to the pathology observed in ERSD (20, 21). Therefore, we also examined the expression of proapoptotic markers in livers of AAV-treated *Pcsk9*$^{-/-}$ mice. Consistent with the observed UPR activation, increased cleaved caspase-3 staining was observed only in the livers of AAV-hLDLR^{G544V}–treated mice (Supplemental Figure 10, A and B). Additional proapoptotic mediators, including poly(ADP-ribose) polymerase (PARP), cleaved PARP, caspases, and cleaved caspases -1, -3, -7, and -9, were also assessed by immunoblot (Supplemental Figure 10C) and real-time PCR (Supplemental Figure 10D), and were exclusively upregulated in the livers of AAV-hLDLR^{G544V}–treated mice.

Fibrosis and inflammation are also strong contributors to the progression of liver disease and injury (13, 22). Thus, the livers of AAV-treated mice were examined for fibrosis via staining of Picrosirius red, α-smooth muscle actin (αSMA), and fibronectin (FN1). The infiltration of CD20-positive inflammatory macrophages was also assessed by IHC staining. Similar to the observed increase in UPR activation and expression of proapoptotic mediators, we observed an increase in the staining of fibrotic and inflammatory markers in the livers of AAV-hLDLR^{G544V}–treated mice compared with AAV-hPCSK9^{Q152H}–treated mice (Supplemental Figure 11, A and B). Heightened expression of the fibrotic markers αSMA, FN1, and TGF-β as well as the inflammatory markers CD4, IL-6, IL-1β, and TNF-α were also observed in this treatment group by immunoblot (Supplemental Figure 11C) and real-time PCR (Supplemental Figure 11D).

ER retention of PCSK9 attenuates LDLR^{G544V}-induced ER stress in mice. So far in the present study, our results revealed that ER retention of PCSK9 protects against ER stress and liver dysfunction, which could potentially be exploited for treating ERSD. Indeed, our own previous reports have shown that ER stress causes the retention of PCSK9 within the ER (34), which may be a physiological protection mechanism. To explore this possibility further, we repeated the AAV experiments in *Pcsk9*$^{+/+}$ mice to analyze the effect on endogenous PCSK9. Consistent with previous reports (8, 9), the expression of ER-retained PCSK9^{Q152H} caused the retention of endogenously expressed mouse PCSK9 (Figure 7A), likely via oligomerization of ER-retained proPCSK9 (5). *Pcsk9*$^{+/+}$ mice treated with AAV-hLDLR^{G544V}, which is also retained in the ER but, in contrast to PCSK9^{Q152H}, induces ER stress, also exhibited a marked

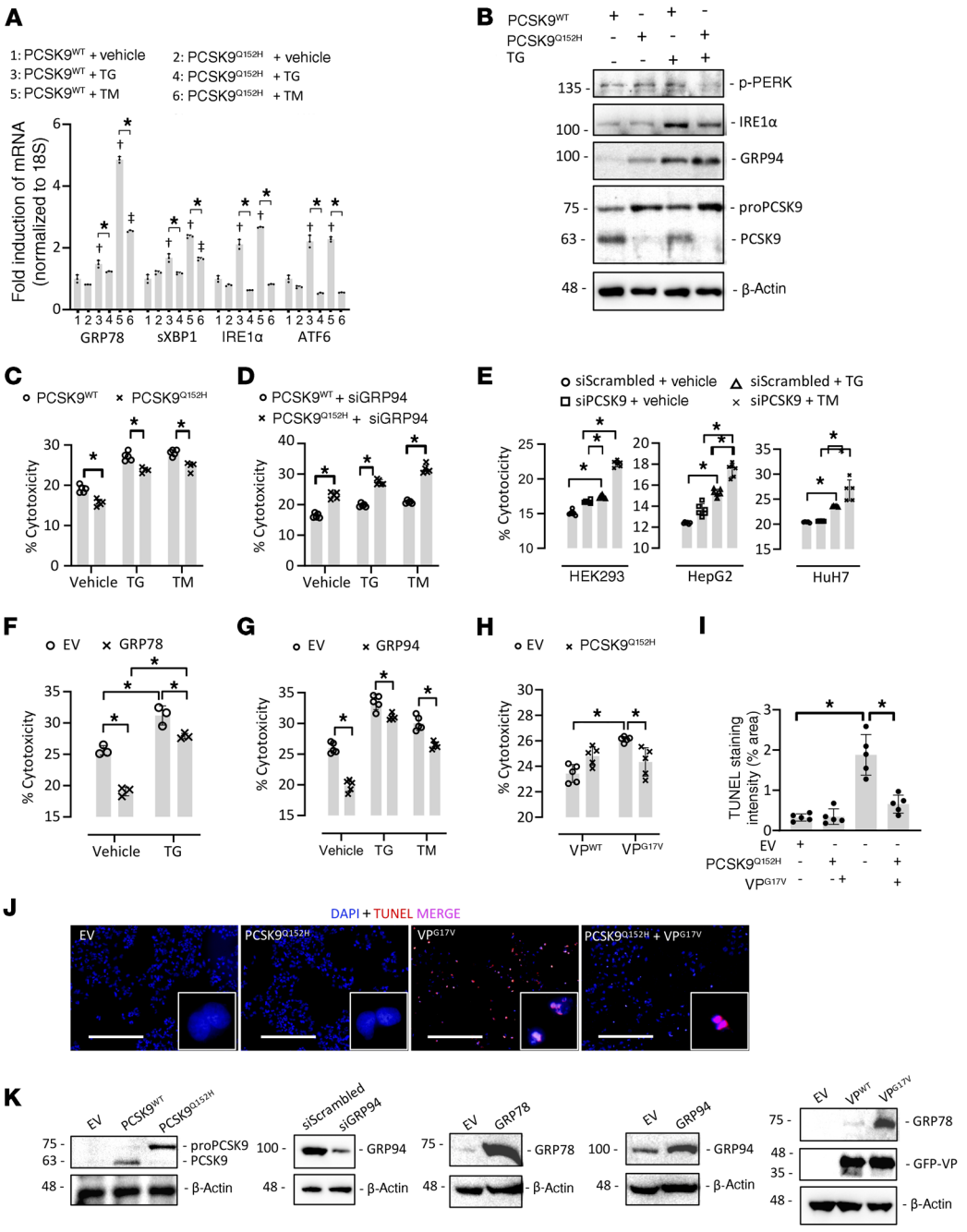

Figure 5. ER PCSK9 retention reduces ER stress–induced cytotoxicity in cultured immortalized hepatocytes. (**A**) HEK293 cells were transfected with plasmids encoding either human PCSK9 WT ($PCSK9^{WT}$) or the ER-retained variant $PCSK9^{Q152H}$ for 48 hours and subsequently treated with the ER stress–inducing agent thapsigargin (TG; 100 nM) or tunicamycin (TM; 2 μg/mL) for an additional 24 hours. ER stress marker expression was assessed by real-time PCR. (**B**) The expression of ER stress markers p-PERK, IRE1α, and GRP94 was also assessed in HuH7 immortalized hepatocytes transfected with either $PCSK9^{WT}$ or $PCSK9^{Q152H}$ in the presence and absence of TG using immunoblots. (**C** and **D**) Cytotoxicity was examined in PCSK9-transfected HepG2 cells in the absence (**C**) or presence (**D**) of siRNA targeted against GRP94 (siGRP94) using an LDH release assay. (**E**) Cytotoxicity was also examined in HEK293, HuH7, and HepG2 cells transfected with siRNA targeted against PCSK9 (siPCSK9) in the presence and absence of TG. (**F** and **G**) The effect of increased GRP78 and GRP94 expression on cytotoxicity caused by ER stress–inducing agents TG (100 nM) and TM (2 μg/mL) was also examined. (**H**) LDH release assays were carried out in HepG2 cells cotransfected with WT arginine vasopressin (VP) or a naturally occurring variant known to cause ER stress and cytotoxicity (VP^{G17V}) in the presence or absence of ER-retained $PCSK9^{Q152H}$. (**I** and **J**) These findings were confirmed by staining of apoptotic DNA damage using a TUNEL assay. (**K**) Effective transfection in HepG2 cells was confirmed using immunoblots. Values are represented as mean ± SD. $^{*}P < 0.05$; $^{\dagger}P < 0.05$ vs. group 1; $^{\dagger\dagger}P < 0.05$ vs. group 2. ANOVA was used for all statistical comparisons (**A**–**J**). Scale bars: **J**, 200 μm.

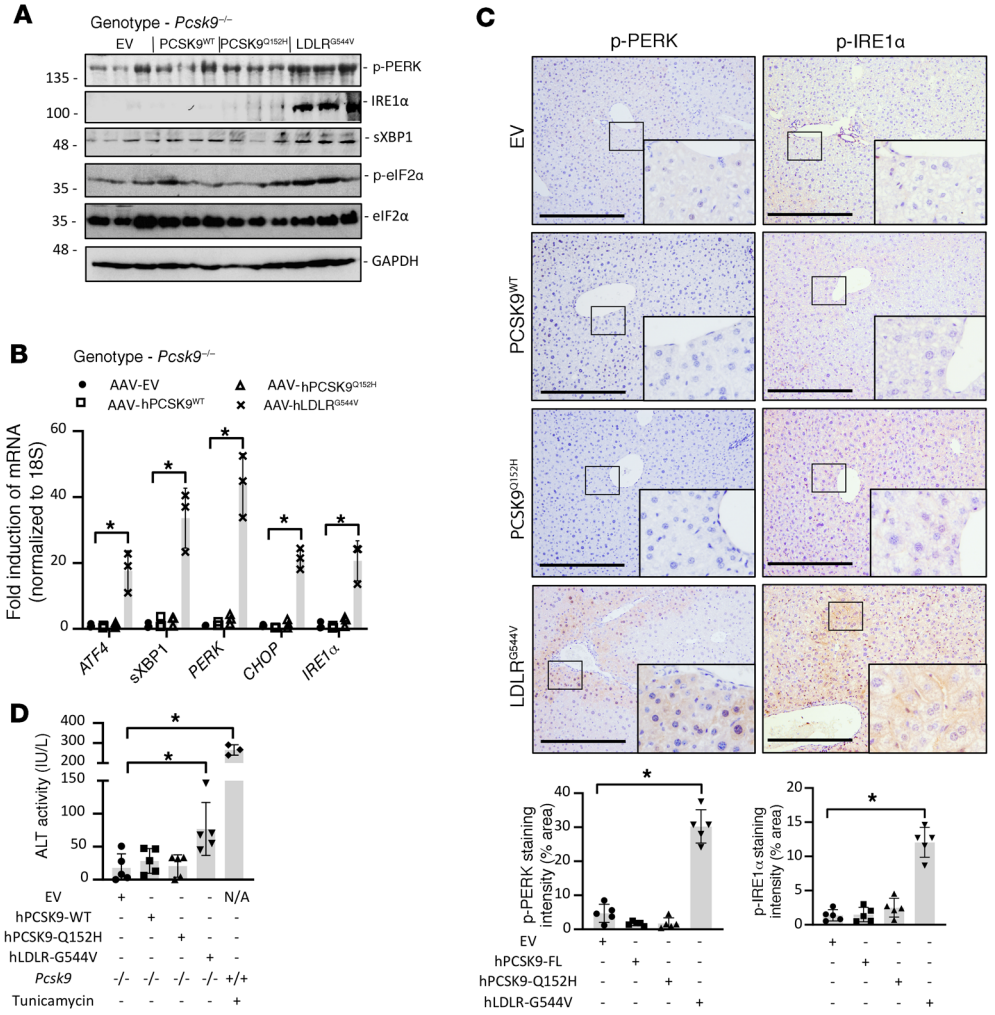

Figure 6. ER retention of hLDLR^{G544V}, but not hPCSK9^{Q152H}, causes a robust UPR activation in liver. (**A** and **B**) The livers of *Pcsk9*$^{-/-}$ mice (n = 5) treated with AAV encoding EV, hPCSK9^{WT}, and ER-retained variants hPCSK9^{Q152H} and hLDLR^{G544V} were examined for expression of UPR markers p-PERK, IRE1α, sXBP1, p-eIF2α, ATF4, and CHOP by immunoblotting and real-time PCR. (**C**) Hepatic p-PERK and p-IRE1α expression was also examined via IHC staining. Staining intensity was quantified using ImageJ software. (**D**) Liver injury was examined in these mice via quantification of serum ALT activity. Values are expressed as mean ± SD. *P < 0.05. ANOVA was used for all statistical comparisons (**A**–**D**). Scale bars: **C**, 200 μm.

reduction in endogenously expressed circulating PCSK9 levels compared with the empty vector control. An increase in hepatic PCSK9 protein was also observed in the livers of AAV-hLDLR^{G544V}–treated *Pcsk9*$^{+/+}$ mice, as determined by ELISA (Figure 7B). PCSK9 mRNA transcript levels in AAV-hLDLR^{G544V}–treated *Pcsk9*$^{+/+}$ mice were unchanged, suggesting that the observed increase in PCSK9 protein in the livers of these mice did not occur as a result of de novo synthesis (Supplemental Figure 12). Notably, consistent with a general protective effect of ER-retained PCSK9, a reduction in LDLR^{G544V}-induced expression of ER stress markers was observed in the livers of the *Pcsk9*$^{+/+}$ mice compared with the *Pcsk9*$^{-/-}$ mice (Figure 7C). Consistent with these data, assessment of liver injury revealed a substantial reduction in ALT activity in AAV-hLDLR^{G544V}–treated *Pcsk9*$^{+/+}$ mice compared with AAV-hLDLR^{G544V}–treated *Pcsk9*$^{-/-}$ mice (Figure 7D). Here, we observed that even endogenously expressed PCSK9 was able to mitigate ER stress caused by an overexpressed LOF LDLR variant. These data further support PCSK9, not only as a functional protein that transits the ER prior to its secretion, but also as an important ER-resident protein with chaperone-like function.

Both AAV-hPCSK9^{Q152H} and AAV-hLDLR^{G544V} were also coadministered to a cohort of *Pcsk9*$^{-/-}$ mice to further assess whether ER retention of hPCSK9^{Q152H} can protect against ER stress. Control groups in this experiment included mice to which either 2 equivalent doses of AAV-EV, or 1 dose of AAV-EV and either hAAV-PCSK9^{Q152H} or hAAV-LDLR^{G544V}, were coadministered. Successful expression of PCSK9^{Q152H} in mice given 2 serial doses of AAV was confirmed by immunoblotting for hepatic proPCSK9 (Figure 7E). Consistent with previous experimental cohorts, increased expression of GRP78 and GRP94 was observed in the livers of dual hPCSK9^{Q152H}- and hLDLR^{G544V}-expressing mice, whereas increased expression of the ER stress markers p-IRE1α, ATF6, and sXBP1 was restricted to those expressing only hLDLR^{G544V}. Notably, these immunoblots also revealed a reduction of ER stress marker abundance in mice coexpressing hPCSK9^{Q152H} and hLDLR^{G544V} compared with those expressing hLDLR^{G544V} alone. Similarly, serum ALT activity was significantly increased in hLDLR^{G544V}-expressing mice but not in those coexpressing hPCSK9^{Q152H} and hLDLR^{G544V} (Figure 7F). Overall, these data demonstrate that PCSK9 is retained in the ER during conditions of ER stress and also reveal that its retention can attenuate liver injury resulting from the expression of the misfolded LDLR^{G544V} variant known to cause ER stress (27).

Circulating anti-GRP78 autoantibodies are elevated in patients with nonalcoholic steatohepatitis, but not in patients expressing

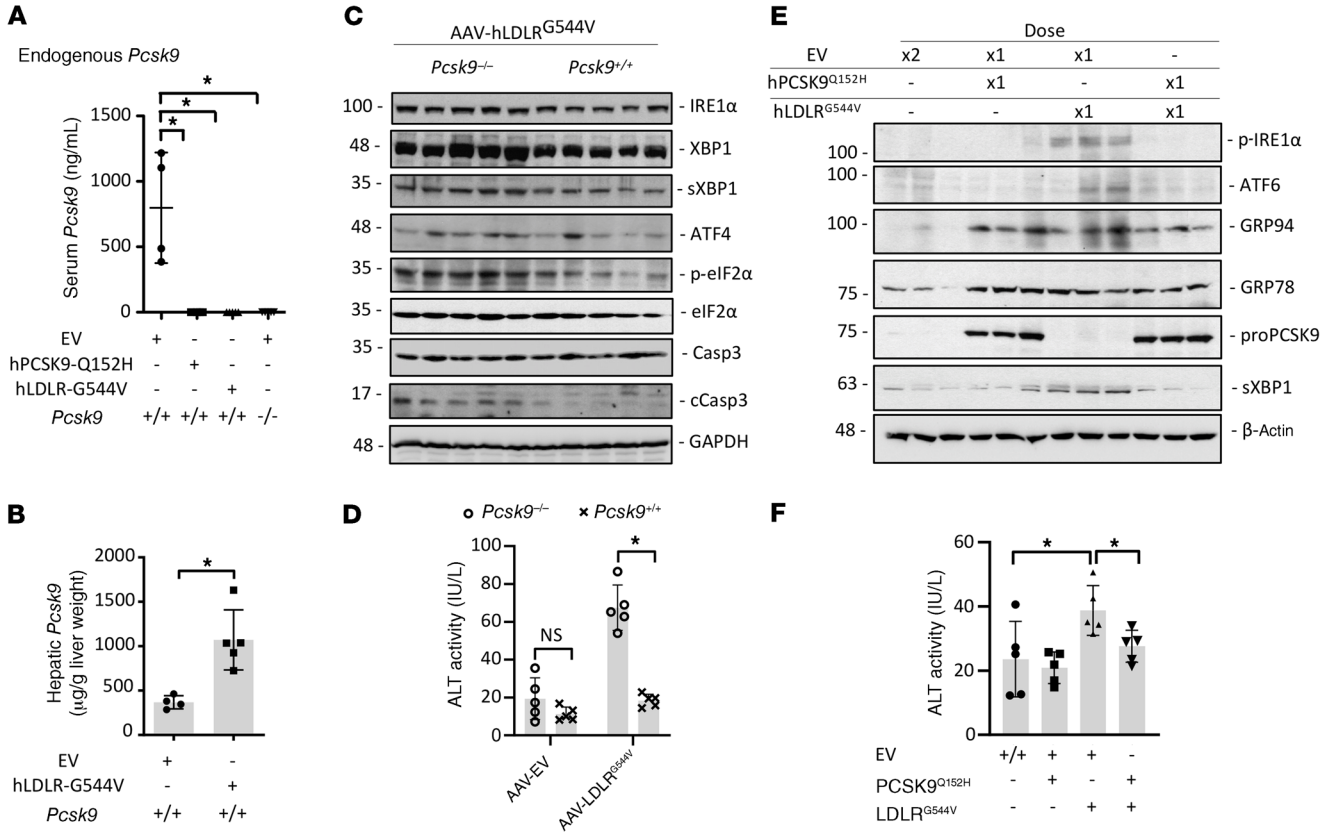

Figure 7. ER retention of PCSK9 protects against hLDLR^{G544V}-induced ER stress. (**A** and **B**) Serum and hepatic PCSK9 levels were examined in *Pcsk9*$^{+/+}$ mice treated with AAV encoding either ER-retained hPCSK9^{Q152H} or hLDLR^{G544V} (n = 5). (**C**) ER stress and apoptosis marker expression were assessed by immunoblotting in the livers of *Pcsk9*$^{-/-}$ and *Pcsk9*$^{+/+}$ mice expressing hLDLR^{G544V}. Casp3, caspase-3; cCasp3, cleaved caspase-3. (**D**) Liver injury was examined in these mice via quantification of serum ALT activity. (**E** and **F**) ER stress marker expression and serum ALT activity was also examined in a cohort of mice (n = 5) cotreated with (a) 2 equivalent doses of AAV-EV; (b) 1 dose of AAV-EV and 1 dose of either AAV-hPCSK9^{Q152H} or AAV-hLDLR^{G544V}; or (c) 1 dose of AAV-hPCSK9^{Q152H} and 1 dose of AAV-hLDLR^{G544V}. Values are represented as mean ± SD. *P < 0.05. ANOVA was used for all statistical comparisons (**A**–**F**).

PCSK9^{Q152H}. Finally, circulating levels of a surrogate marker of ER stress were examined in the serum of healthy human volunteers carrying the PCSK9^{Q152H} variation. During conditions of prolonged ER stress, ER-resident GRP78 can localize to the cell surface, where it plays a variety of roles as a prosurvival signaling molecule with implications in cancer progression and atherosclerosis (30–32, 35). In line with these studies, hepatocytes in the livers of AAV-hLDLR^{G544V}–treated mice, as well as hepatocytes in the livers of TM-treated mice, exhibited increased cell surface GRP78 expression (Supplemental Figure 6). Following the expression of this neoantigen at the cell surface, the immune system can generate autoantibodies targeted against surface GRP78. Because this process is dependent on ER stress, we used circulating anti-GRP78 autoantibodies as a surrogate marker of systemic ER stress in subjects harboring the PCSK9^{Q152H} variation. Validating our choice of marker, a modest yet significant increase in autoantibody titers was observed in patients with nonalcoholic steatohepatitis (NASH) (Figure 8A), a progressive form of liver disease in which ER stress is a well-established and causative driver (13, 22). Thus, ER stress–driven liver disease can increase circulating levels of anti-GRP78 autoantibodies. However, individuals expressing ER-retained PCSK9^{Q152H} did not exhibit increased levels of anti-GRP78 autoantibodies (Figure 8B). Taken together, these data suggest that lifelong ER retention of PCSK9^{Q152H} does not trigger hepatic ER stress in humans.

Discussion

ERSD encompasses a variety of etiologies, most of which are caused by heritable genetic variations in secretory or cell surface proteins that transit the ER (12, 14–17). Owing to the occurrence of symptoms in ERSD patients, several of these diseases have been characterized to date. It is likely, however, that many individuals harboring LOF proteins that are retained in the ER remain asymptomatic and thus many important genetic variations have yet to be discovered. Here, we characterize a rare instance in which a protein that is retained in the ER not only fails to trigger toxicity but actually protects against it. Thus, we identified a cochaperone function for ER-retained PCSK9^{Q152H} that increases the abundance of GRP78 and GRP94, thereby protecting against ER stress–induced liver injury.

In support of our experimental findings and working hypothesis, other proteins that promote resistance against ER stress and liver injury by interacting with GRP78 and GRP94 have indeed been identified. For instance, Gupta and colleagues have identified Bag5 as an ER-resident GRP78 binding partner capable of increasing its stability and expression at the protein level in

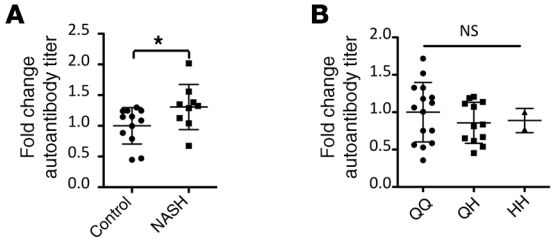

Figure 8. Circulating anti-GRP78 autoantibodies are elevated in the blood of patients with NASH, but not in carriers of the PCSK9^{Q152H} variation. (**A**) ELISAs were used to measure plasma levels of anti-GRP78 autoantibodies in healthy controls (n = 12) and in patients with NASH (n = 9). (**B**) Anti-GRP78 autoantibodies were then examined in the plasma of heterozygous (QH; n = 12) and homozygous (HH; n = 2) carriers of the PCSK9^{Q152H} mutation as well as in noncarrier WT family siblings (QQ; n = 15). Values are expressed as mean ± SD. *P < 0.05. ANOVA was used for all statistical comparisons (**A** and **B**).

cardiomyocytes (36). Consistent with our observations, overexpression of Bag5 reduced cell death whereas siRNA-mediated knockdown had the opposite effect. GALNT6 was also identified as an O-type glycosyltransferase capable of increasing the protein stability of GRP78 and suppressing ER stress–induced apoptosis (37). To increase the clinical applicability of the findings outlined in this study, further research must be conducted in order to determine whether the benefit associated with ER retention of PCSK9 is limited to the Q152H variant. Interestingly, it is now well established that PCSK9 autocatalytic cleavage following passage through the translocon occurs spontaneously, following nearly zero-order kinetics (38). Given that (a) our findings demonstrate that WT cleavable PCSK9 can also protect against ER stress, and (b) this form of PCSK9 likely exists in its mature/cleaved state following its entry into the lumen of the ER, it is possible, and perhaps even likely, that either form of PCSK9 could interact with GRP78 to protect against ER stress. Thus, the benefits of the PCSK9^{Q152H} variant may also be reproduced among those expressing the WT secreted PCSK9 using small-molecule inhibitors of PCSK9 autocatalytic cleavage.

Given the well-established prosurvival/protective role of GRP78, it is not surprising that proteins that increase its stability also confer protection against ER stress–inducing stimuli. Accumulating evidence now suggests that GRP94, similarly to GRP78, also plays a significant protective role (39, 40). In support of this possibility, recent evidence has demonstrated that (a) the knockdown of GRP94 is embryonic lethal (39), (b) GRP94 knockout in embryonic stem cells leads to compensatory changes in UPR signaling/activation (40), which often leads to increased susceptibility to cytotoxicity (41), and (c) liver-specific deletion of GRP94 leads to liver injury and spontaneous hepatocellular carcinoma in aged mice (42). Likewise, overexpression of these chaperones is also known to protect against ER stress (39, 43).

Our previous findings demonstrated that conditions of ER stress, via pharmacologic intervention, cause the retention of PCSK9 in the ER of hepatocytes and reduce its levels in circulation (34). We now report that overexpression of LDLR^{G544V}, which causes severe ER stress and liver injury in *Pcsk9*$^{-/-}$ mice, also abolished the circulating levels of endogenously expressed mouse PCSK9 in *Pcsk9*$^{+/+}$ mice. Given that hepatic PCSK9 protein levels are increased in AAV-hLDLR^{G544V}–treated mice compared with AAV-EV–treated controls, and that mRNA transcript levels are not affected, these data suggest that PCSK9 is being retained in the livers of these mice as a result of ER stress. Given the use of a liver-targeted AAV serotype in our studies, these data are also consistent with liver-specific *Pcsk9* ablation studies demonstrating that circulating PCSK9 originates almost exclusively from liver hepatocytes (44). The previously documented dominant-negative effect of ER-retained PCSK9^{Q152H} on secreted levels of endogenously expressed mouse WT PCSK9 was also observed in our studies (8, 9). Finally, in a manner consistent with our findings in cultured cells, the cellular retention of PCSK9 in the livers of AAV-hLDLR^{G544V}–treated *Pcsk9*$^{+/+}$ mice caused a reduction of ER stress marker expression in comparison with mice expressing the same LDLR variant that lack PCSK9 (AAV-hLDLR^{G544V}–treated *Pcsk9*$^{-/-}$). Collectively, these results suggest that the retention of PCSK9 in hepatocytes during conditions of ER stress mitigates UPR activation and subsequent liver injury.

Anti-PCSK9 antibody therapeutics markedly reduce plasma LDLc in patients at high risk of cardiovascular events (45). Given the impressive LDL-lowering efficacy of PCSK9 inhibition, and the prevalence of the underlying disease against which this strategy is targeted, the need for additional PCSK9-inhibitory treatment modalities is well justified (38, 46, 47). Currently, pharmacologic inhibition of PCSK9 proteolysis to induce its retention in the ER has proven to be a major challenge. Although PCSK9 autocatalytic cleavage represents the rate-limiting step of PCSK9 secretion and stands out as a classical pharmacologic target, this process follows exceedingly fast kinetics and is concealed from pharmacologic agents by 2 lipid bilayers (38). However, given the appealing nature of low-cost small-molecule inhibitors of PCSK9, this highly sought-after target is still being actively pursued in academia and industry (48, 49).

Beyond the role of proPCSK9 as a putative cochaperone for hepatic GRP78 and GRP94, our biochemical, genetic, and clinical evidence suggest that inhibition of proPCSK9 autocatalytic cleavage in the ER may represent a safe and unique approach for the management of hyperlipidemia as well as having the added benefit of preventing liver dysfunction. The experimental findings and clinical observations described in this study indicate that the uncleaved proPCSK9 is an important player in ER stress response. In further support of this conclusion, we have recently demonstrated that *Pcsk9*$^{-/-}$ mice exhibit increased ER stress, inflammation, insulin resistance, and liver injury in response to an ER stress–inducing HFD, compared with *Pcsk9*$^{+/+}$ mice (50). Although individuals harboring variations in *PCSK9* that reduce its abundance in the ER or those treated with *PCSK9* gene silencing therapies appear healthy, our data suggest that intracellular PCSK9 may play an important role in maintaining the functionality of the UPR. To our knowledge, this is the first example of a single variation of a human gene, already beneficial against CVD risk, that may also offer additional protection against a major group of liver-related diseases. The evolutionary cost of this putative beneficial variation (if any) through the process of natural selection in humans remains an open question to be addressed by further experimental studies. The translational tools generated in this work will certainly be useful for further

mechanistic investigations in the progression of liver diseases and in the discovery of therapeutic interventions for the treatment of these disorders.

Methods

Carriers and noncarriers of PCSK9^{Q152H}. Samples were collected after participants fasted for 12 hours and abstained from consuming alcohol for 48 hours. Plasma samples were separated by ultracentrifugation and aliquoted and stored at –80°C. Standard assays of plasma biochemistry were performed by a certified laboratory (Biron Health Group).

Plasma samples from NASH patients. Plasma samples from healthy volunteers and patients with NASH were purchased from Discovery Life Sciences. All samples were acquired from male volunteers/patients over the age of 50 years.

Liver MRI. MRI was performed on a 3T system (Magnetom Skyra, Siemens). 3D dual-echo spoiled gradient recalled echo (VIBE) phase-sensitive 2-point Dixon sequences were acquired for separation of whole-body water and fat. Two-dimensional multi-echo spoiled gradient recalled echo sequences with 7-echo readout were acquired during a single breath hold to cover the entire liver for calculation of fat fraction along a dynamic scale from 0 to 50%.

Design and generation of AAV vector constructs. PCSK9 and LDLR variant cDNA was inserted between a bovine growth hormone poly(A) and an elongation factor 1a promoter. A mammalian expression cassette was subsequently inserted and flanked by inverted terminal repeats of AAV. HEK293 T cells were then transfected with the resulting construct and recombinant AAV was collected, as described previously (51). Briefly, 8×10^8 cells were lysed in 8 mL of serum-free DMEM through 3 rounds of freeze/thaw. AAV-containing lysate was then treated and loaded onto AVB Sepharose columns (Cytiva). Following elution with pH 3.0 glycine HCl, acidic pH was promptly neutralized with 1 M Tris-HCl and dialyzed using PBS containing 1 mM $MgCl_2$ and 2.5 mM KCl. Slid-A-Lyzer Concentration Solution (Thermo Fisher Scientific) was then used to concentrate the isolated AAV in the dialysis cassette. The QuickTiter AAV Quantification Kit (Cell Biolabs Inc.) was then used to titer and quantify purified AAV particles. The parental AAV serotype 8 was used in these studies for optimal liver expression (*27*).

Translational mouse model and AAV administration. AAV injections were carried out in male *Pcsk9*$^{-/-}$ mice on the C57BL/6J background ($n = 5$) and in *Pcsk9*$^{+/+}$ on the C57BL/6J background ($n = 5$). Mice had access to water and normocaloric diet (NCD) ad libitum and were maintained in rooms with 12-hour light/12-hour dark cycles. Mice were injected with 1 dose of AAV (4.5×10^{12} vector genomes) at 8 weeks of age and sacrificed at 12 weeks of age. The 4 AAV treatment groups were AAV-hPCSK9^{WT}, AAV-hPCSK9^{Q152H}, AAV-hLDLR^{G544V}, and AAV-EV control. A third cohort of male mice ($n = 5$ per group) also received coadministration of (a) 2 equivalent doses of AAV-EV; (b) 1 dose of AAV-EV and 1 dose of either AAV-hPCSK9^{Q152H} or AAV-hLDLR^{G544V}; or (c) 1 dose of AAV-hPCSK9^{Q152H} and 1 dose of AAV-hLDLR^{G544V}.

Mouse studies involving the feeding of a HFD were carried out at McMaster University and performed in strict accordance with the institutional animal ethics guidelines. Male *Pcsk9*$^{-/-}$ mice on a C57BL/6J background and age-matched C57BL/6J *Pcsk9*$^{+/+}$ controls ($n = 5$; The Jackson Laboratory) were started on either HFD or NCD diet at 6 weeks of age for a duration of 12 weeks. These mice were also housed in rooms with 12-hour light/12-hour dark cycles.

Cell culture, treatments and transfections. HepG2 cells (ATCC, HB-8065), HEK293 cells (CRL-1573, ATCC), and HuH7 cells (generated in-house) were grown in DMEM (Gibco, Thermo Fisher Scientific) supplemented with 10% (vol/vol) FBS (MilliporeSigma) and 50 U/mL of penicillin and streptomycin (MilliporeSigma). Cells were seeded in 6-well cell culture dishes to a confluence of 60% and transfected 24 hours later. The transfection cocktail consisted of 1 μg DNA, 3 μL X-tremeGENE HP DNA reagent (MilliporeSigma), and 100 μL Opti-MEM (Gibco, Thermo Fisher Scientific) per well of cells containing 1 mL complete DMEM. The cDNA of human *PCSK9* or its corresponding Q152H variant was cloned into pIRES-EGFP (Clontech), and a V5 tag was inserted between the N-terminal signal peptide (residues 1–30) and the start of the prosegment, as described previously (8). Human GRP78 and GRP94 cDNA were cloned into the pcDNA3.1 vector. Small interfering RNA targeted against GRP94 (SMARTpool siGenome HSP90B1) and PCSK9 (SMARTpool siGenome PCSK9) were purchased from Dharmacon and transfected using RNAiMAX (Thermo Fisher Scientific). Cells were incubated in the transfection cocktail for 24 hours, and medium was subsequently replaced with fresh DMEM containing 1% FBS for an additional 48 hours prior to lysis or assessment of cytotoxicity with LDH release assays. For assessment of ER stress and/or ER stress–induced cytotoxicity, cells were treated with vehicle (containing equimolar DMSO), TG (300 nM), or TM (2 μg/mL) 24 hours before lysis.

Immunoblots and protein quantification. Small fragments of fresh, flash-frozen mouse livers (0.05 g) were lysed in SDS-containing buffer and normalized to total protein before being electrophoretically resolved on polyacrylamide gels. Resolved proteins were then transferred to nitrocellulose membranes, blocked in skim milk, and exposed to primary antibodies overnight (18 hours) on a gentle rocker at 4°C. Unbound primary antibodies were subsequently removed via Tris-buffered saline (TBS) washes. Immunoblots were then incubated in horseradish peroxidase–conjugated (HRP-conjugated) secondary antibodies, developed using chemiluminescent reagent (FroggaBio), and quantified using a Bio-Rad Imaging system with immunoblots reprobed against β-actin or GAPDH. Immunoblot quantifications are presented in Supplemental Tables 2–8. Commercial antibodies used for immunoblots are shown in Supplemental Table 9. See complete unedited blots in the supplemental material.

Real-time PCR. Liver RNA was collected using RNeasy Mini Kits (QIAGEN) and normalized to 2 μg before being reverse-transcribed to cDNA using SuperScript VILO cDNA synthesis kit (Life Technologies). The viia7 system (Thermo Fisher Scientific) in conjunction with FAST SYBR Green (Life Technologies) was used for quantitative real-time PCR assessment of mRNA species in each sample with specific primer sets (Supplemental Table 10).

Quantification of serum GRP78 autoantibodies. Autoantibodies were detected by ELISA as described previously (33). Briefly, 96-well plates coated with a KLH-conjugated GRP78-specific peptide (CNVSKDSC) were blocked in PBS-Tween containing 3% BSA. Serum samples diluted 1:100 were added to the plates and incubated for 18 hours. Excess sample was then removed via washing, and the plate was subsequently exposed to alkaline phosphatase–conjugated anti-human IgG and developed using alkaline phosphatase substrate at a wavelength of 405 nm in a standard spectrophotometer (Molecular Devices).

IHC and immunofluorescent staining of paraffin-embedded tissue. IHC was conducted as described previously (25, 35). Briefly, 4-μm-thick paraffin-embedded mouse liver or adipose tissue sections were stained with primary antibodies overnight (18 hours). Sections were then stained with biotinylated secondary antibodies and streptavidin-HRP. Exposure to NovaRED peroxidase kit for 5 minutes or less permitted the visualization of analyte antibody complexes. Thioflavin-S staining was also carried out in paraffin-embedded tissues. After deparaffinization, sections were exposed to a 1% filtered aqueous solution of thioflavin-S (MilliporeSigma) for 10 minutes and subsequently washed in 80% ethanol. Slides were mounted in aqueous mount and imaged immediately to avoid photobleaching. All images were taken with a high-powered light microscope and processed and/or quantified using ImageJ software (NIH). For quantification purposes, several images were taken from the livers of each mouse using a ×20 objective and staining intensity measured with a fixed pixel-density threshold between groups. Commercial antibodies used for IHC are shown in Supplemental Table 9.

LDH and TUNEL assays in cultured cells. Transfected cells were incubated in DMEM containing 1% FBS 24 hours before LDH release assays. Assay was carried out per the manufacturer's instructions (Roche). TUNEL staining of apoptotic nuclei in transfected HuH7 cells was also carried out per the manufacturer's instructions (Trevigen). Briefly, HuH7 cells were fixed in paraformaldehyde and permeabilized in TBS containing 0.02% Triton-X. Cells were then incubated with the TdT labeling enzyme at 37°C for 1 hour and subsequently incubated in 594-labeled streptavidin. Cells were visualized using a fluorescent microscope (EVOS, Life Technologies) and quantified using ImageJ software (NIH).

Quantitative assessment of plasma ALT activity, triglyceride/cholesterol levels, and circulating PCSK9. Examination of plasma ALT (Cayman Chemical), triglycerides (Wako Diagnostics), and cholesterol (Wako Diagnostics) was carried out using colorimetric assays and serum/hepatic PCSK9 levels via ELISA (R&D Systems).

Statistics. All values are expressed as mean with SD indicated by error bars. Statistical analysis was done for 2-group comparisons using the unpaired, 2-tailed Student's *t* test, and for comparisons involving multiple groups using 1-way ANOVA. Differences between groups were considered statistically significant at P less than 0.05.

Study approval. All subjects fully agreed to the study protocol and signed a consent form, which was approved by the Montreal Clinical Research Institute (Montreal, Canada) ethics committee. Mouse studies conducted at Amgen Inc. were approved by Amgen's Institutional Animal Care and Use Committee. Mouse studies conducted at McMaster University were approved and conducted in strict accordance with the institutional animal ethics guidelines.

Author contributions

PFL, BA, SJ, AP, MC, RP, WA, NGS, and RCA contributed to study conception, experimental design, and analysis. JD, SS, BA, and SJ carried out mouse studies with AAV vectors. JHB, KP, AAAH, and KDW contributed to data collection and interpretation. PFL, RCA, and MC wrote the manuscript, and JHB, KP, BA, SJ, WGR, MC, HW, GP, RP, WA, and NGS assisted with manuscript editing. MC discovered the human PCSK9^{Q152H} mutation and initiated clinical studies. MC, HW, and MM designed the clinical protocol, directed its implementation, and analyzed and interpreted the results. AT programmed the MRI and analyzed and interpreted the images.

Acknowledgments

We thank David R. Cool (Department of Pharmacology and Toxicology, Boonshoft School of Medicine, Wright State University) for the vasopressin expression plasmids. We also thank Hellen Pickersgill (Life Science Editors) for editing the manuscript. This work was supported in part by research grants to RCA from the Heart and Stroke Foundation of Ontario (T-6146), the Heart and Stroke Foundation of Canada (G-13-0003064 and G-15-0009389), and the Canadian Institutes of Health Research (CIHR) (FRN 67116,173520); to NGS from the Leducq Foundation (13 CVD 03), a CIHR Foundation grant (no. 148363), and a Canada Research Chair (no. 216684); and to MC from La Fondation J-Louis Lévesque and the Richard and Edith Straus–Aclon Foundation. RP and WA received research support from the Gillson-Longenbaugh Foundation. Financial support from The Research Institute of St. Joe's Hamilton and Amgen Canada is also acknowledged. RCA is a Career Investigator of the Heart and Stroke Foundation of Ontario and holds the Amgen Canada Research Chair in the Division of Nephrology at St. Joseph's Healthcare and McMaster University.

Address correspondence to: Richard C. Austin, St. Joseph's Healthcare Hamilton, 50 Charlton Avenue E., Hamilton, Ontario, Canada L8N 4A6. Phone: 905.522.1155 ext. 35175; Email: austinr@taari.ca. Or to: Michel Chrétien, Clinical Research Institute of Montreal, 110, des Pins Avenue West, Montréal, Québec, Canada H2W 1R7. Phone: 514.987.5664; Email: michel.chretien@ircm.qc.ca. Or to: Wadih Arap, Rutgers Cancer Institute of New Jersey, 205 South Orange Avenue, Newark, New Jersey 07101, USA. Email: wadih.arap@rutgers.edu.

1. Ference BA, et al. Low-density lipoproteins cause atherosclerotic cardiovascular disease. 1. Evidence from genetic, epidemiologic, and clinical studies. A consensus statement from the European Atherosclerosis Society Consensus Panel. *Eur Heart J*. 2017;38(32):2459–2472.
2. Huynh K. Lipids: very low achieved LDL-cholesterol levels improve cardiovascular outcomes. *Nat Rev Cardiol*. 2017;14(11):630–631.
3. Fernandez-Ruiz I. Atherosclerosis: should we redefine the 'normal' LDL-cholesterol range? *Nat Rev Cardiol*. 2018;15(2):68–69.
4. Abifadel M, et al. Mutations and polymorphisms in the proprotein convertase subtilisin kexin 9 (PCSK9) gene in cholesterol metabolism and disease. *Hum Mutat*. 2009;30(4):520–529.
5. Seidah NG, et al. The secretory proprotein convertase neural apoptosis-regulated convertase 1 (NARC-1): liver regeneration and neuronal differentiation. *Proc Natl Acad Sci U S A*. 2003;100(3):928–933.
6. Maxwell KN, Breslow JL. Adenoviral-mediated expression of Pcsk9 in mice results in a low-density lipoprotein receptor knockout phenotype. *Proc Natl Acad Sci U S A*. 2004;101(18):7100–7105.
7. Cohen JC, Boerwinkle E, Mosley TH Jr., Hobbs HH. Sequence variations in PCSK9, low LDL, and protection against coronary heart disease. *N Engl J Med*. 2006;354(12):1264–1272.
8. Mayne J, et al. Novel loss-of-function PCSK9 variant is associated with low plasma LDL cholesterol in a French-Canadian family and with impaired processing and secretion in cell culture. *Clin Chem*. 2011;57(10):1415–1423.
9. Benjannet S, Hamelin J, Chrétien M, Seidah NG. Loss- and gain-of-function PCSK9 variants: cleavage specificity, dominant negative effects, and low density lipoprotein receptor (LDLR) deg-

radation. *J Biol Chem*. 2012;287(40):33745–33755.
10. Chrétien M, Mbikay M. 60 years of POMC: from the prohormone theory to pro-opiomelanocortin and to proprotein convertases (PCSK1 to PCSK9). *J Mol Endocrinol*. 2016;56(4):T49–T62.
11. Kim I, Xu W, Reed JC. Cell death and endoplasmic reticulum stress: disease relevance and therapeutic opportunities. *Nat Rev Drug Discov*. 2008;7(12):1013–1030.
12. Oakes SA, Papa FR. The role of endoplasmic reticulum stress in human pathology. *Annu Rev Pathol*. 2015;10:173–194.
13. Lebeaupin C, Vallée D, Hazari Y, Hetz C, Chevet E, Bailly-Maitre B. Endoplasmic reticulum stress signalling and the pathogenesis of non-alcoholic fatty liver disease. *J Hepatol*. 2018;69(4):927–947.
14. Carlson J. Endoplasmic reticulum storage disease. *Histopathology*. 1990;16(3):309–312.
15. Austin RC. The unfolded protein response in health and disease. *Antioxid Redox Signal*. 2009;11(9):2279–2287.
16. Yan Z, Hoffmann A, Kaiser EK, Grunwald WC, Cool DR. Misfolding of mutated vasopressin causes ER-retention and activation of ER-stress markers in Neuro-2a cells. *Open Neuroendocrinol J*. 2011;4:136–146.
17. Rutishauser J, Spiess M. Endoplasmic reticulum storage diseases. *Swiss Med Wkly*. 2002;132(17-18):211–222.
18. Teckman JH, Perlmutter DH. Retention of mutant alpha(1)-antitrypsin Z in endoplasmic reticulum is associated with an autophagic response. *Am J Physiol Gastrointest Liver Physiol*. 2000;279(5):G961–G974.
19. Lin L, Schmidt B, Teckman J, Perlmutter DH. A naturally occurring nonpolymerogenic mutant of alpha 1-antitrypsin characterized by prolonged retention in the endoplasmic reticulum. *J Biol Chem*. 2001;276(36):33893–33898.
20. Hetz C. The unfolded protein response: controlling cell fate decisions under ER stress and beyond. *Nat Rev Mol Cell Biol*. 2012;13(2):89–102.
21. Faitova J, Krekac D, Hrstka R, Vojtesek B. Endoplasmic reticulum stress and apoptosis. *Cell Mol Biol Lett*. 2006;11(4):488–505.
22. Dara L, Ji C, Kaplowitz N. The contribution of endoplasmic reticulum stress to liver diseases. *Hepatology*. 2011;53(5):1752–1763.
23. Malhi H, Gores GJ. Molecular mechanisms of lipotoxicity in nonalcoholic fatty liver disease. *Semin Liver Dis*. 2008;28(4):360–369.
24. Poirier S, Mamarbachi M, Chen WT, Lee AS, Mayer G. GRP94 regulates circulating cholesterol levels through blockade of PCSK9-induced LDLR degradation. *Cell Rep*. 2015;13(10):2064–2071.
25. Lebeau P, et al. Loss-of-function PCSK9 mutants evade the unfolded protein response sensor GRP78 and fail to induce endoplasmic reticulum stress when retained. *J Biol Chem*. 2018;293(19):7329–7343.
26. Fang CC, Wu CF, Liao YJ, Huang SF, Chen M, Chen YA. AAV serotype 8-mediated liver specific GNMT expression delays progression of hepatocellular carcinoma and prevents carbon tetrachloride-induced liver damage. *Sci Rep*. 2018;8(1):13802.
27. Sørensen S, Ranheim T, Bakken KS, Leren TP, Kulseth MA. Retention of mutant low density lipoprotein receptor in endoplasmic reticulum (ER) leads to ER stress. *J Biol Chem*. 2006;281(1):468–476.
28. Poirier S, et al. The proprotein convertase PCSK9 induces the degradation of low density lipoprotein receptor (LDLR) and its closest family members VLDLR and ApoER2. *J Biol Chem*. 2008;283(4):2363–2372.
29. Zhu G, Lee AS. Role of the unfolded protein response, GRP78 and GRP94 in organ homeostasis. *J Cell Physiol*. 2015;230(7):1413–1420.
30. Crane ED, et al. Anti-GRP78 autoantibodies induce endothelial cell activation and accelerate the development of atherosclerotic lesions. *JCI Insight*. 2018;3(24):99363.
31. Zhang Y, Liu R, Ni M, Gill P, Lee AS. Cell surface relocalization of the endoplasmic reticulum chaperone and unfolded protein response regulator GRP78/BiP. *J Biol Chem*. 2010;285(20):15065–15075.
32. Zhang XX, et al. The cell surface GRP78 facilitates the invasion of hepatocellular carcinoma cells. *Biomed Res Int*. 2013;2013:917296.
33. Al-Hashimi AA, et al. Binding of anti-GRP78 autoantibodies to cell surface GRP78 increases tissue factor procoagulant activity via the release of calcium from endoplasmic reticulum stores. *J Biol Chem*. 2015;290(48):28725.
34. Lebeau P, et al. Endoplasmic reticulum stress and Ca^{2+} depletion differentially modulate the sterol regulatory protein PCSK9 to control lipid metabolism. *J Biol Chem*. 2017;292(4):1510–1523.
35. Al-Hashimi AA, et al. Binding of anti-GRP78 autoantibodies to cell surface GRP78 increases tissue factor procoagulant activity via the release of calcium from endoplasmic reticulum stores. *J Biol Chem*. 2010;285(37):28912–28923.
36. Gupta MK, et al. GRP78 interacting partner Bag5 responds to ER stress and protects cardiomyocytes from ER stress-induced apoptosis. *J Cell Biochem*. 2016;117(8):1813–1821.
37. Lin J, Chung S, Ueda K, Matsuda K, Nakamura Y, Park JH. GALNT6 stabilizes GRP78 protein by O-glycosylation and enhances its activity to suppress apoptosis under stress condition. *Neoplasia*. 2017;19(1):43–53.
38. Seidah NG, Prat A, Pirillo A, Catapano AL, Norata GD. Novel strategies to target proprotein convertase subtilisin kexin 9: beyond monoclonal antibodies. *Cardiovasc Res*. 2019;115(3):510–518.
39. Marzec M, Eletto D, Argon Y. GRP94: an HSP90-like protein specialized for protein folding and quality control in the endoplasmic reticulum. *Biochim Biophys Acta*. 2012;1823(3):774–787.
40. Mao C, et al. Targeted mutation of the mouse Grp94 gene disrupts development and perturbs endoplasmic reticulum stress signaling. *PLoS One*. 2010;5(5):e10852.
41. Lebeau P, Byun JH, Yousof T, Austin RC. Pharmacologic inhibition of S1P attenuates ATF6 expression, causes ER stress and contributes to apoptotic cell death. *Toxicol Appl Pharmacol*. 2018;349:1–7.
42. Chen WT, et al. Liver-specific knockout of GRP94 in mice disrupts cell adhesion, activates liver progenitor cells, and accelerates liver tumorigenesis. *Hepatology*. 2014;59(3):947–957.
43. Suyama K, et al. Overexpression of GRP78 protects glial cells from endoplasmic reticulum stress. *Neurosci Lett*. 2011;504(3):271–276.
44. Zaid A, et al. Proprotein convertase subtilisin/kexin type 9 (PCSK9): hepatocyte-specific low-density lipoprotein receptor degradation and critical role in mouse liver regeneration. *Hepatology*. 2008;48(2):646–654.
45. Sabatine MS, et al. Evolocumab and clinical outcomes in patients with cardiovascular disease. *N Engl J Med*. 2017;376(18):1713–1722.
46. Latimer J, Batty JA, Neely RD, Kunadian V. PCSK9 inhibitors in the prevention of cardiovascular disease. *J Thromb Thrombolysis*. 2016;42(3):405–419.
47. Sabatine MS, Underberg JA, Koren M, Baum SJ. Focus on PCSK9 inhibitors: from genetics to clinical practice. *Postgrad Med*. 2016;128(suppl 1):31–39.
48. Chorba JS, Galvan AM, Shokat KM. Stepwise processing analyses of the single-turnover PCSK9 protease reveal its substrate sequence specificity and link clinical genotype to lipid phenotype. *J Biol Chem*. 2018;293(6):1875–1886.
49. Chorba JS, Shokat KM. The proprotein convertase subtilisin/kexin type 9 (PCSK9) active site and cleavage sequence differentially regulate protein secretion from proteolysis. *J Biol Chem*. 2014;289(42):29030–29043.
50. Lebeau PF, et al. *Pcsk9* knockout exacerbates diet-induced non-alcoholic steatohepatitis, fibrosis and liver injury in mice. *JHEP Rep*. 2019;1(6):418–429.
51. Xiong Y, et al. Long-acting MIC-1/GDF15 molecules to treat obesity: evidence from mice to monkeys. *Sci Transl Med*. 2017;9(412):eaan8732.